

SU-8 thick photoresist processing as a functional material for MEMS applications

This article has been downloaded from IOPscience. Please scroll down to see the full text article.

2002 J. Micromech. Microeng. 12 368

(<http://iopscience.iop.org/0960-1317/12/4/303>)

View [the table of contents for this issue](#), or go to the [journal homepage](#) for more

Download details:

IP Address: 131.252.130.248

The article was downloaded on 05/02/2013 at 07:03

Please note that [terms and conditions apply](#).

SU-8 thick photoresist processing as a functional material for MEMS applications

Ewan H Conradie and David F Moore

Engineering Department, Cambridge University, Trumpington Street, Cambridge
CB2 1PZ, UK

E-mail: e.h.conradie.98@cantab.net

Received 10 January 2002, in final form 18 April 2002

Published 13 June 2002

Online at stacks.iop.org/JMM/12/368

Abstract

The use of SU-8 high aspect ratio, thick, photoresist as a functional material for MEMS applications is described in this paper. SU-8 processing is developed to implement low-stress SU-8 structures as permanent and functional material incorporated with silicon-on-insulator technologies. Silicon micromachined cantilevers were fabricated with SU-8 structures on the cantilevers as added masses. Separation of material function can be achieved in this way. Silicon provides excellent mechanical properties, while SU-8 is used as extra mass to adjust the mechanical behaviour. The resonance behaviour of the cantilever structure with SU-8 is characterized through measurement, simulation and calculation, and the strength of the SU-8 material for this purpose is evaluated. The results show that SU-8 is well suited as a permanent material in mechanically active MEMS devices, and several applications are suggested. 3D MEMS architectures can also be achieved in this manner.

1. Introduction

The SU-8 photoresist is a negative, thick, epoxy-photoplastic, high aspect ratio resist. It finds application in several MEMS areas, including the fabrication of plastic micromolds or metal micromolds by electroplating [1], microfluidics for SU-8 microchannels [2], fabrication of photoplastic structures such as microgears [3], microcoil fabrication [4], rapid prototyping using laser machining and as a bonding material for optical components [5]. SU-8 is a UV sensitive resist which can be spin coated in a conventional spinner in thicknesses ranging from 1 μm to 300 μm , while up to 2 mm thicknesses can be obtained by multilayer coatings. Combined with standard lithographic processes, SU-8 offers excellent opportunities in MEMS applications and packaging.

The properties and processing parameters of SU-8 have been described by various groups [6–8]. SU-8 has very suitable properties of thickness and chemical stability, and has some good mechanical and optical properties as well. However, despite all these advantages, the SU-8 photoresist suffers from three disadvantages, namely adhesion selectivity, stress and resist stripping.

SU-8 adhesion is good on materials such as silicon and gold [6], but on other materials such as glass, nitrides, oxides and other metals, the adhesion is poor and the resist easily delaminates from such material surfaces during development. Adhesion can be improved on certain surfaces by using a suitable adhesion promoter, or by using additives to the SU-8.

On many suitable surfaces for spinning SU-8 such as silicon or glass, the thermal expansion coefficient mismatch is large (SU-8 has a thermal expansion coefficient of 52 ppm K^{-1} compared to silicon which has a coefficient of 3 ppm K^{-1}). This causes large amounts of stress at the material interface due to shrinkage of the resist while crosslinking during curing. This stress effect is pronounced in large SU-8 structures, and if poor adhesion is obtained during processing, the photoresist delaminates easily. Low thermal expansion coefficient SU-8 resist can somewhat alleviate this problem.

As a photoplastic material, SU-8 is chemically stable and resistant to most acids and other solvents. Consequently, it is difficult to remove once crosslinked, and suitable methods of stripping, compatible with other materials in the structure, are often not effective or desirable to use. Recent advances by

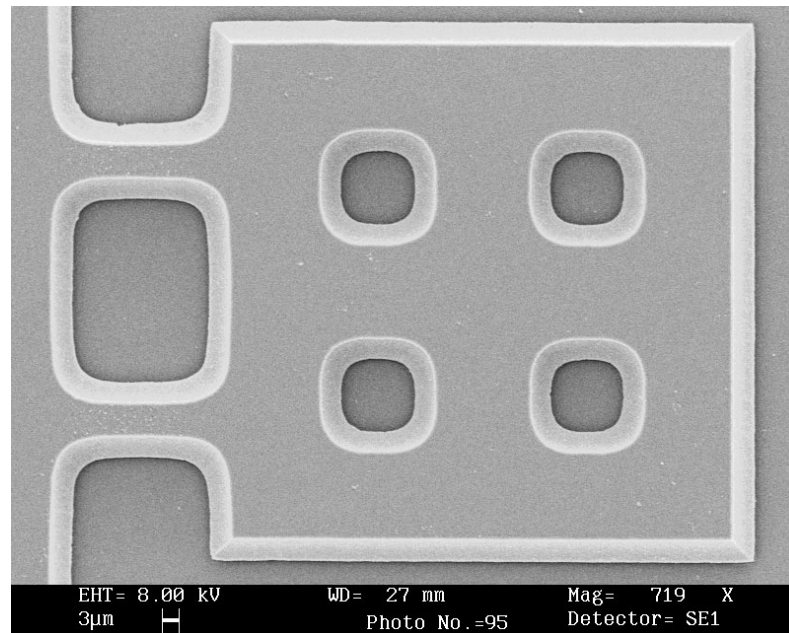


Figure 1. SEM image of a SOI cantilever without any SU-8 structures.

Sotec Microsystems [9] have somewhat alleviated this problem by producing a SU-8 stripper.

However, these three disadvantages lend themselves well to certain MEMS applications where it is not desired to remove the resist. Small, and hence low-stress, SU-8 structures patterned with good adhesion on silicon can be used as functional or permanent material when combined with conventional MEMS processes and materials.

This paper reports silicon-on-insulator (SOI) cantilevers which have been fabricated to investigate the use of SU-8 as a functional material. Small SU-8 pillars are fabricated on top of these cantilevers as added masses. The structure itself derives its mechanical properties from the silicon material, while the SU-8 structures allow modification of the structure's mass and mechanical behaviour, such as resonance frequency. A suitable SU-8 process was developed for this investigation. Figure 1 shows a plan view scanning electron microscope (SEM) image of a cantilever without any SU-8 structures.

2. SOI and SU-8 processing

The silicon cantilevers were fabricated in the form of arrays of cantilevers using silicon-on-insulator material (SOI) with an 8 μm thick top silicon layer and a 2 μm thick silicon dioxide sacrificial layer.

Lithography was performed using AZ5218 photoresist to pattern the cantilevers. A reactive ion etch (RIE) process using a SF_6 , CF_4 and O_2 plasma was used to etch the silicon. A partial buffered HF etch for 5 min was performed next to clean the silicon surface in preparation for SU-8 coating with good adhesion. SU-8 50 from MicroChem Corporation [10] was used to spin coat the sample at 2000 rpm for 60 s. This results in a coating thickness of 30 μm . The sample is then given sufficient relaxation time of a few hours to allow reflow to complete and to prevent problems with step coverage on the silicon cantilevers.

A pre-exposure bake is performed using temperature ramping to reduce stress. The sample is baked on a hotplate for 10 min at 50 $^\circ\text{C}$, then ramped up to 85 $^\circ\text{C}$ over a period of 5 min and finally allowed to bake at 85 $^\circ\text{C}$ for 35 min. The pre-exposure bake is deliberately extended to allow maximum solvent evaporation. Exposure is performed using UV illumination of 16 mW cm^{-2} for 100 s through a second mask defining the locations of the SU-8 on the cantilever. The SU-8 structures on the cantilevers are simple square pillars ranging between 5 μm and 15 μm in size. A total of up to nine pillars were placed on a cantilever, and different configurations of the SU-8 placement were used to investigate the influence of SU-8 pillar arrangement.

Post-exposure baking is performed under the same conditions as the pre-exposure bake. This bake is also extended to ensure maximum crosslinking which results in good strength for the SU-8 structures for use as a functional material. Developing was performed in undiluted PGMEA for 2–3 min until done. The sample is then rinsed in isopropanol and dried using nitrogen gas. Rinsing in de-ionized water results in a minor chemical reaction between the water and the PGMEA which destroys small SU-8 pillars.

Undercutting of the silicon dioxide is done in a 1:1 solution of concentrated HF and buffered HF. Finally, an aluminium metal layer was thermally evaporated onto the sample to form the contacts for electrostatic actuation during measurement. External contacts are made by using conventional soldering techniques. Figure 2 shows a SEM image of the array of cantilevers with SU-8 pillars fabricated on top of the cantilevers while figure 3 shows a schematic cross-section diagram of the complete process flow.

3. Theory and simulation

The effectiveness of using SU-8 as a functional material is tested by considering the resonance frequency of the cantilever

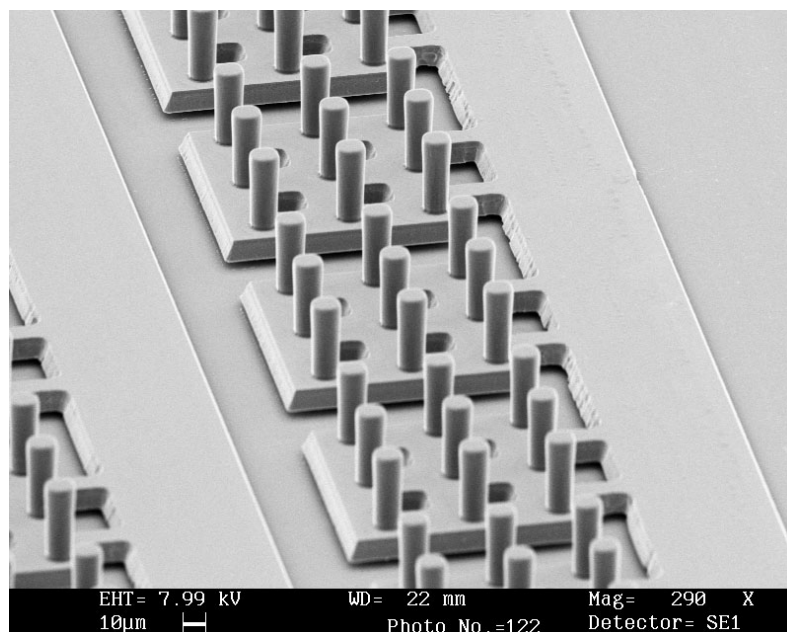


Figure 2. SU-8 pillars fabricated on an array of silicon cantilevers. The pillars are $10 \times 10 \mu\text{m}^2$ in size and $30 \mu\text{m}$ high.

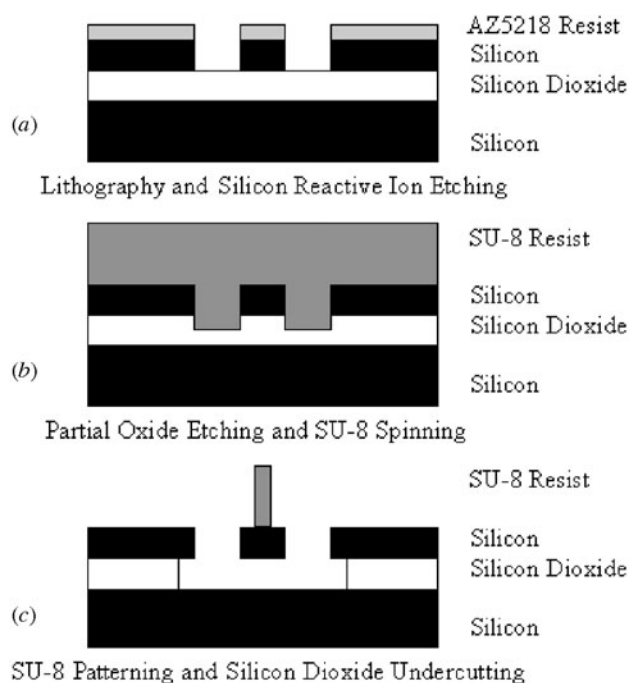


Figure 3. Schematic cross-section process flow diagram for a cantilever with SU-8 structures.

structure. Placement of the added SU-8 pillars as mass will change the resonance behaviour of the structure, and at maximum resonance amplitude (limited to $4 \mu\text{m}$ peak to peak by the sacrificial silicon dioxide thickness) the strength of the material can be tested due to the two silicon layers impacting at a rate equivalent to the resonance frequency at high resonance amplitudes.

Theoretically, the cantilever structure can be modelled as a two-component system. The first part is a massless spring

component formed by the two spring supports and a rigid cantilever of length dependant on the location of the centre of mass. The second part is a mass component and consists of the rigid paddle structure and the holes which aid in the etching. Due to the facts that (i) the cantilever undercut is not considered, (ii) the dimensional changes due to the RIE are not considered and (iii) the fact that the rigid paddle structure is not entirely rigid (it is a flexible extension of the two beam support), this model gives higher results (561.5 kHz) than those obtained by measurement and simulation. However, the model is useful to determine the influence of dimensional parameter changes on the resonance frequency.

By adding SU-8 structures to the cantilever, the SU-8 pillars add mass and mass moment of inertia around the centre of mass, and change the position of the centre of mass depending on the location of the SU-8 pillars. Theoretical calculation shows that three $10 \times 10 \mu\text{m}^2$ pillars ($30 \mu\text{m}$ high) placed at the front of the cantilever result in a resonance frequency of 523.7 kHz , while three similar pillars placed at the back of the cantilever result in a resonance frequency of 553.9 kHz . The influence of pillar location can clearly be seen as important. Cantilevers with added SU-8 all resonate at frequencies lower than cantilevers without SU-8. Theoretical calculations have shown that for a nine-pillar configuration, the resonance frequency of the cantilever is not linear (it is linear for small changes in the pillar cross-sectional dimensions) with an increase in the cross-sectional dimension or size of the square SU-8 pillars.

Simulations of the resonance frequencies of the cantilever structures were performed using FEMGV [11] and ABAQUS [12]. As the RIE process changes the shape and size of the structure, the simulations were performed by using accurate dimensions of the cantilevers obtained using SEM micrographs. Trapezoidal shapes in the cantilever can be replaced by rectangular sections of equal volume without changing the resonance behaviour. (The rigid paddle section

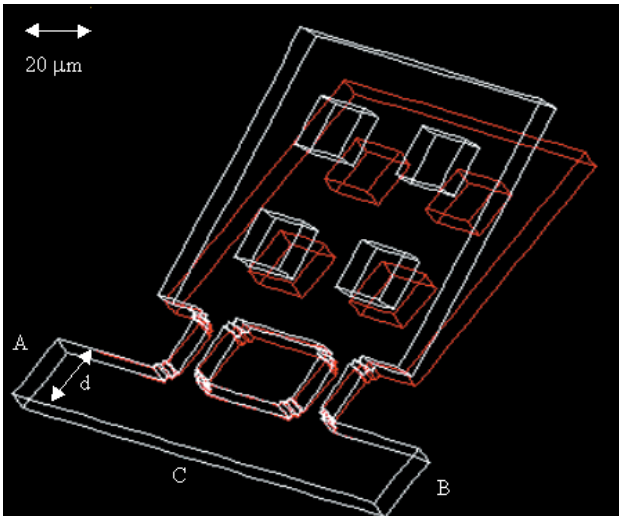


Figure 4. ABAQUS simulation of the cantilever structure without SU-8, incorporating RIE dimension changes and undercut of the support banks. The structure is clamped at locations A, B and C. Length d is the length of the undercut.

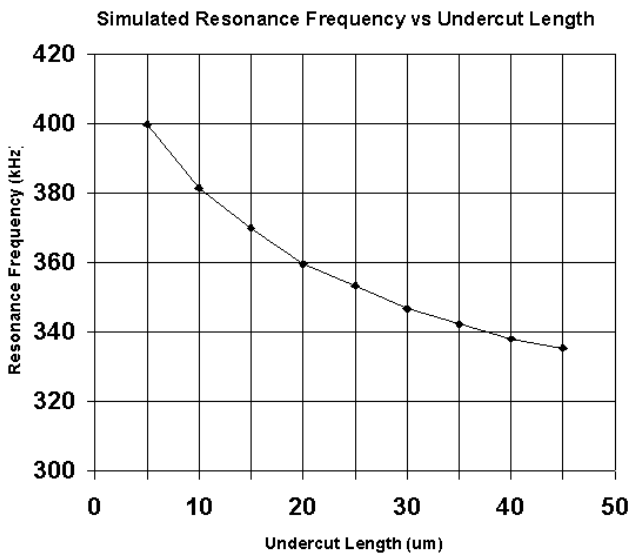


Figure 5. Simulated first-order resonance frequency as a function of the length of the undercut (see figure 4).

is essentially just a large mass.) The simulations also incorporated the effect of the length of the undercut support bank. This is of particular importance, as the HF undercutting of the silicon dioxide is not uniform throughout the sample, resulting in different undercuts for cantilevers at different locations. Figure 4 shows the first-order resonance frequency mode for the cantilever without SU-8. The resonance frequency is 353.4 kHz, which is associated with a HF undercut of approximately 25 μm , which was estimated from the experimental work. Figure 5 shows the simulation results for a physical cantilever for different undercut lengths of the support banks.

The resonance frequency results are all lower than theoretical values for reasons mentioned earlier. As shown in figure 5, the resonance frequency changes less with a change in

Table 1. Simulated cantilever resonance frequency results for $10 \times 10 \mu\text{m}^2$ SU-8 pillars (30 μm high) for different numbers and arrangements of the SU-8 structures. A '=' indicates the two spring support beams of the cantilever while the circles indicate SU-8 locations. The geometry of the simulated cantilever is as shown in figure 1.

SU-8 arrangement and number of pillars	Simulated first-order resonance frequency
0 =	357.3 kHz
3 = $\begin{matrix} \circ & & \circ \\ \circ & & \circ \end{matrix}$	354.5 kHz
3 = $\begin{matrix} \circ & & \circ \\ \circ & & \circ \end{matrix}$	343.1 kHz
3 = $\begin{matrix} \circ & & \circ \\ \circ & & \circ \end{matrix}$	325.9 kHz
6 = $\begin{matrix} \circ & \circ & \circ \\ \circ & \circ & \circ \end{matrix}$	340.6 kHz
7 = $\begin{matrix} \circ & \circ & \circ \\ \circ & \circ & \circ \end{matrix}$	331.1 kHz
9 = $\begin{matrix} \circ & \circ & \circ \\ \circ & \circ & \circ \end{matrix}$	314.2 kHz

Table 2. Simulated cantilever resonance frequency results for $5 \times 5 \mu\text{m}^2$ SU-8 pillars (30 μm high) for different numbers and arrangements of the SU-8 structures.

SU-8 arrangement and number of pillars	Simulated first-order resonance frequency
0 =	357.3 kHz
4 = $\begin{matrix} \circ & \circ \\ \circ & \circ \end{matrix}$	348.8 kHz
5 = $\begin{matrix} \circ & \circ \\ \circ & \circ \end{matrix}$	347.8 kHz
6 = $\begin{matrix} \circ & \circ \\ \circ & \circ \end{matrix}$	347.5 kHz
7 = $\begin{matrix} \circ & \circ \\ \circ & \circ \end{matrix}$	344.9 kHz
8 = $\begin{matrix} \circ & \circ \\ \circ & \circ \end{matrix}$	346.3 kHz
9 = $\begin{matrix} \circ & \circ \\ \circ & \circ \end{matrix}$	343.7 kHz

the undercut for very large undercuts, than for small undercuts where the change in resonance frequency can be significant for a given change in undercut length. This result can be useful to ensure that all the cantilevers in an array resonate at approximately the same frequency. The resonance frequencies of cantilevers deliberately undercut further will not be as susceptible to HF undercutting variations during processing. Figure 6 shows a SEM image of two cantilevers that have holes placed in the support bank to deliberately undercut the structure further by a given amount. Measurement results for this structure on four different cantilevers at different locations on the same substrate resulted in resonance frequencies at 218.1 kHz, 218.4 kHz, 218.2 kHz and 218.9 kHz. These variations are significantly smaller than those found for general cantilevers in an array (between 330 kHz and 340 kHz).

Simulation results obtained for the resonance frequencies of cantilevers with SU-8 pillars fabricated on top are shown in tables 1 and 2. Simulations were performed for both $5 \times 5 \mu\text{m}^2$ and $10 \times 10 \mu\text{m}^2$ pillars that were 30 μm high. The results of the simulations based on the SU-8 pillar placement for three SU-8 pillars agree well with the expected behaviour obtained by theoretical modelling.

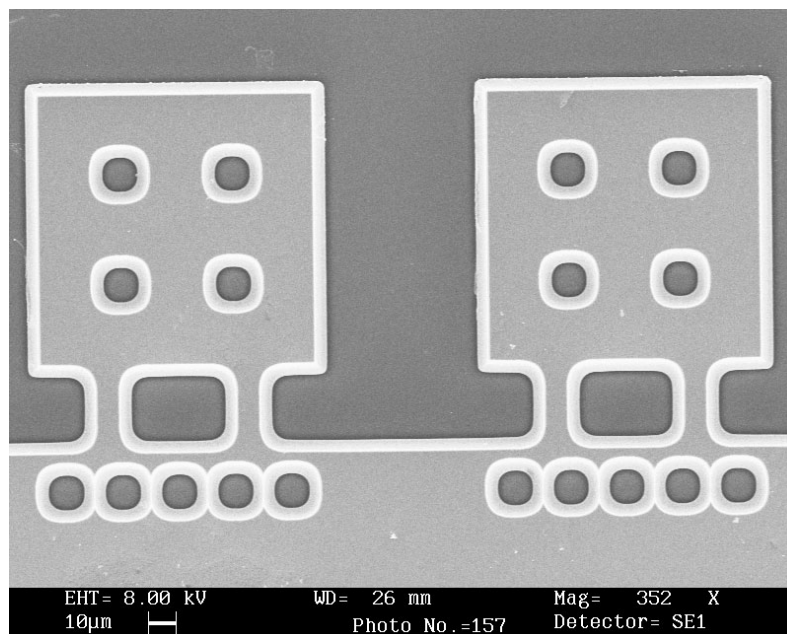


Figure 6. SEM image of cantilevers with fixed additional undercut to deliberately undercut the cantilevers further. The holes reduce the resonance frequency as well.

4. Measurements and discussion

Measurements were performed in a scanning electron microscope (SEM) using electrostatic actuation (superimposed ac and dc voltages are applied to all the cantilevers simultaneously on the top silicon layer, while the silicon substrate is grounded) to measure the resonance frequencies in vacuum [13]. The variation of the electrostatic force is not exactly linear with ac voltage (it is a function of the cantilever–substrate separation distance), generating harmonics in the force applied to the cantilevers. The second- and third-order resonance modes are high (simulated at 1.4 MHz and 3.4 MHz, respectively), and only the first-order mode is relevant.

Figure 7 shows a cantilever without SU-8 actuated (*a*) away from and (*b*) at resonance (342.8 kHz). The actuation voltage is 10 V in conjunction with a 4 V peak to peak ac signal. The resonance frequency increases by a fraction of a kHz if the dc voltage is lowered.

Measurements of the shape of the resonance curve can be performed by sweeping frequency while an image is slowly scanned in the SEM. Using this method, curves can be obtained that show the resonance behaviour with upward sweeping and downward sweeping in frequency. The resonance curves are non-harmonic (possibly due to a non-harmonic drive, or the fact that the trapezoidally shaped spring elements of the fabricated device have unequal cross-sectional stiffness when bending) for the deflections involved, but the response becomes harmonic as the ac signal voltage is reduced to 2 V peak to peak and the deflections in the cantilever beam are small. Figure 8 shows a typical example of a SEM image that is obtained when measuring the shape of the resonance curve. The frequency is swept linearly downwards from 337.9 kHz at C, to 336.4 kHz at A. The resonance amplitude builds up slowly with decreasing frequency, until it drops to zero at B and frequency 337.1 kHz.

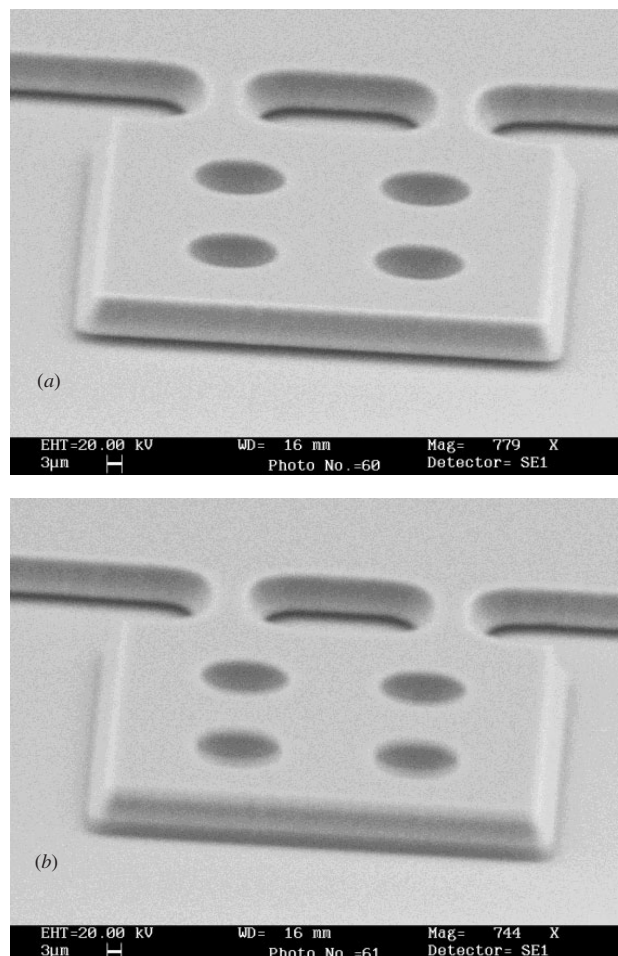


Figure 7. SEM images of a cantilever (*a*) away from and (*b*) at resonance.

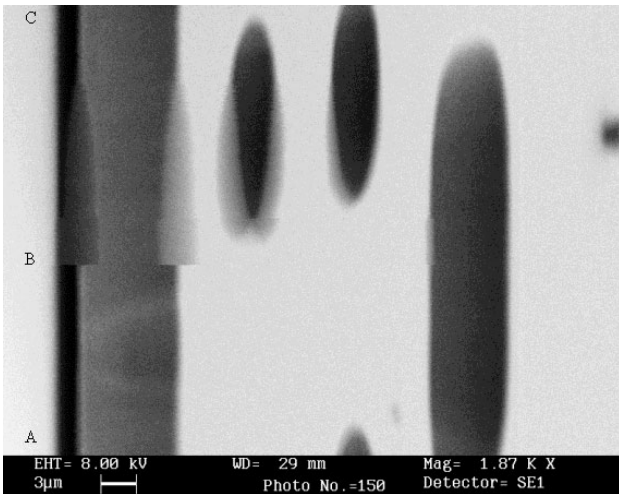


Figure 8. SEM image that is scanned as the frequency is swept to enable measurement of the shape of the resonance curve.

Table 3. Measured cantilever resonance frequency results for $10 \times 10 \mu\text{m}^2$ SU-8 pillars ($30 \mu\text{m}$ high) for different numbers and arrangements of the SU-8 structures.

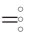
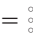
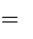
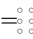
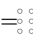
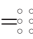
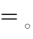
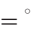
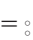
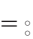
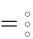
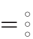
SU-8 arrangement and number of pillars	Measured first-order resonance frequency
0 =	342.8 kHz
3 = 	338.6 kHz
3 = 	321.6 kHz
3 = 	314.5 kHz
6 = 	321.9 kHz
7 = 	315.0 kHz
9 = 	304.6 kHz

Table 4. Measured cantilever resonance frequency results for $5 \times 5 \mu\text{m}^2$ SU-8 pillars ($30 \mu\text{m}$ high) for different numbers and arrangements of the SU-8 structures.

SU-8 arrangement and number of pillars	Measured first-order resonance frequency
0 =	342.8 kHz
4 = 	332.1 kHz
5 = 	330.3 kHz
6 = 	327.4 kHz
7 = 	325.6 kHz
8 = 	323.2 kHz
9 = 	320.3 kHz

Similar measurements were performed to determine the resonance frequency of the cantilevers with SU-8 structures in different sizes and different arrangements. Here the cantilevers were allowed to resonate for extended periods (half an hour to an hour) of time at maximum resonance amplitude of $2 \mu\text{m}$. This results in the cantilever impacting the silicon substrate

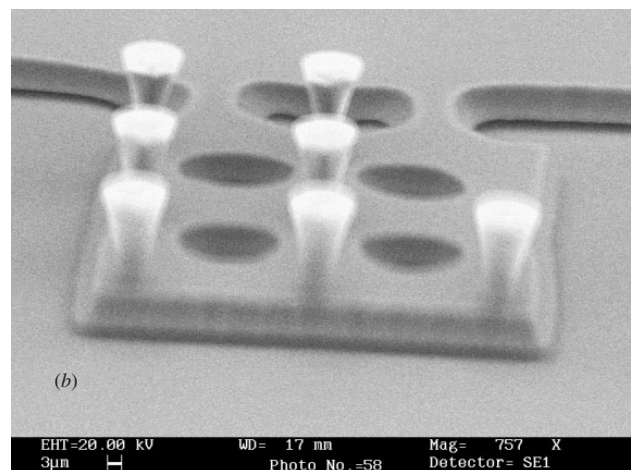
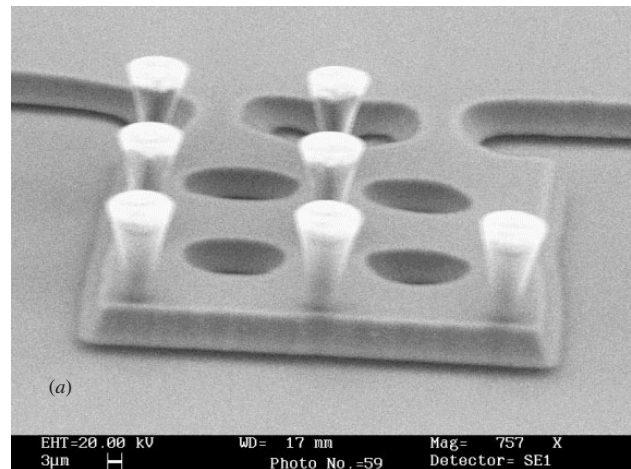


Figure 9. A cantilever with SU-8 pillars (a) away from and (b) at resonance.

at a rate equivalent to the resonance frequency. This rigorous impacting does not dislodge the SU-8 pillars, showing that they are strong enough to withstand mechanical resonance, and small impacting forces. Tables 3 and 4 summarize the results obtained during measurements of $5 \times 5 \mu\text{m}^2$ SU-8 pillars and $10 \times 10 \mu\text{m}^2$ SU-8 pillars. These results were measured for similar arrangements as those simulated (see tables 1 and 2) to enable easy comparison of the results. The measured results are slightly lower than the simulated results, due to uncertainties in the undercut length, cantilever dimensions due to RIE, SU-8 dimensions and the SU-8 density which is dependant on the crosslinking.

The resonance behaviour obtained through measurement shows good correlation to those results obtained through simulation. The expected behaviour of the resonance frequency as a function of the SU-8 pillar placement is once again very similar to theoretical and simulated behaviour. SU-8 pillars placed at the front or free end of the cantilever results in a larger influence on the resonance frequency than SU-8 placed at the back or clamped end of the cantilever. In general, placing SU-8 on a micromachined cantilever results in a decrease in the resonance frequency of the cantilever. Figure 9 shows a silicon-on-insulator cantilever with seven SU-8 pillars (a) away from and (b) at resonance. The SU-8 aspect ratio here is low due to overexposure during processing.

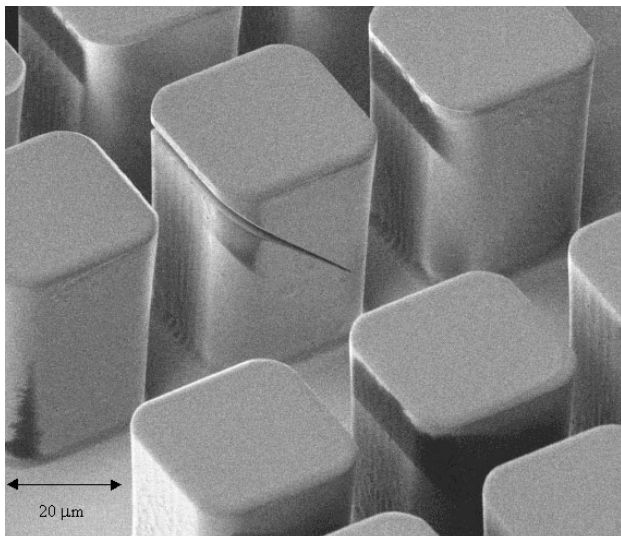


Figure 10. SU-8 pillars on a silicon wafer that are cut using a focused ion beam.

SU-8 provides an excellent way to modify or enhance the behaviour of MEMS structures. Apart from the fact that it is easy to pattern on non-planar surfaces, patterned SU-8 photoplastic structures can also be trimmed by using a laser or focused ion beam (FIB) as shown in figure 10. Potential applications of the SU-8 technology developed in this paper and other general applications include the use in flow sensing as drag walls (adding the third dimension to an otherwise planar, microscale device—current flow sensors are generally macroscale devices), in inertial sensor applications for accelerometers and gyroscopes (as added masses to enhance sensitivity, at the expense of cross-sensitivity, or to modify the resonance modes of a gyroscopic structure in order to bring the Coriolis modes closer together in frequency), for vacuum packaging (SU-8 is dense and easy to pattern), for ferromagnetic magnets by mixing the SU-8 with magnetic powders (SU-8 provides the means to place micromagnets anywhere on a device) and as lenses due to optical transparency, or protective coatings (in conjunction with silicon carbide, diamond-like carbon or other similar materials).

5. Conclusions

These results show that SU-8 as an epoxy-polymer photoresist is well suited for use as a functional material. The use of small SU-8 structures reduces stress, while silicon material provides good adhesion. Strength tests by impacting the cantilevers against the substrate during resonance show that the SU-8 is strong enough to withstand external forces, and

that the adhesion is good. As a functional material SU-8 can be used to adjust the mechanical properties of MEMS devices as shown, and, because silicon surface micromachined structures are inherently planar, adding SU-8 gives the added benefit of moving the device into the third dimension. SU-8 is clearly a material well suited to MEMS applications as a functional part of a micromachined device.

Acknowledgment

The authors would like to thank Alan Heaver for valuable assistance during the scanning electron microscope (SEM) measurements performed for this work.

References

- [1] Lorentz H, Despont M, Fahrni N, Brugger J, Vettiger P and Renaud P 1998 High-aspect-ratio, ultrathick, negative-tone near UV photoresist and its applications for MEMS *Sensors Actuators A* **64** 33
- [2] Guerin L J, Bossel M, Demierre M, Calmes S and Renaud P 1997 Simple and low cost fabrication of embedded microchannels by using a new thick-film photoplastic *Proc. Transducers '97 (Chicago, USA)* p 1419
- [3] Bertsch A, Lorentz H and Renaud P 1999 3D microfabrication by combining microstereolithography and thick UV lithography *Sensors Actuators A* **73** 14
- [4] Seidemann V, Bütetfisch S and Büttgenbach S 2001 Application and investigation of in-plane compliant SU-8 structures for MEMS *Proc. Transducers '01 (Munich, Germany)* p 1616
- [5] O'Brien J, Hughes P J, Riordan A O, Driscoll C O, Shu-Ren Y, Alderman J, Lane B and O'Neill B 2000 Advanced photoresist technologies for MST *11th Micromechanics Europe Workshop (MME '00) (Uppsala, Sweden)* p B7
- [6] Lorentz H, Despont M, Fahrni N, LaBlance N, Renaud P and Vettiger P 1997 SU-8: a low cost negative resist for MEMS *J. Micromech. Microeng.* **7** 121
- [7] Lorentz H, Laudon M and Renaud P 1998 Mechanical characterisation of a new high-aspect-ratio near UV resist *Microelectron. Eng.* **41-42** 371
- [8] Zhang J, Tan K L, Hong G D, Yang L J and Gong H Q 2001 Polymerisation optimisation of SU-8 photoresist and its applications in microfluidic systems and MEMS *J. Micromech. Microeng.* **11** 20
- [9] Sotec Microsystems, Switzerland webpage <http://www.somisys.ch>
- [10] MicroChem Corporation, USA webpage <http://www.microchem.com>
- [11] Femsys Limited, United Kingdom webpage <http://www.femsys.co.uk>
- [12] Hibbit, Karlsson and Sorenson Incorporated, USA webpage <http://www.hks.com>
- [13] Burns D J and Helbig H F 1999 A system for automated electrical and optical characterisation of microelectromechanical devices *IEEE J. Microelectromech. Syst.* **8** 473